# An experimental study on tool wear behaviour in micro milling of nano Mg/Ti metal matrix composites

**Xiangyu Teng[1], Dehong Huo[1,2*], Islam Shyha[3], Wanqun Chen[1], Eugene Wong[1]**

1 Mechanical Engineering, School of Engineering, Newcastle University, Newcastle Upon Tyne, NE1 7RU, UK
2 The State Key Laboratory of Mechanical Transmission, Chongqing University, Chongqing 400044, China
3 Department of Mechanical and Construction Engineering, Northumbria University at Newcastle; Newcastle upon Tyne, NE1 8ST, UK

*Correspondence: dehong.huo@newcastle.ac.uk; Tel.: +44-191-208-6230

## Abstract

With the development of MMCs, the mechanical properties of MMCs with small volume fraction of nano-sized particles were found to be even superior to that with larger content of micron-sized particles. However, the improved mechanical properties of MMCs bring tremendous challenges such as premature tool failure Tiin machining process. This study exhibits an investigation on tool wear in micro milling of magnesium based MMCs reinforced with 1.98 Vol.% of nano-sized titanium particles using 0.5mm diameter two-flute tungsten carbide micro endmills. The tool wear was characterised both quantitatively and qualitatively by observing tool wear patterns and analysing the effect of cutting parameters on flank wear, reduction in tool diameter, cutting forces, surface roughness, and burr formation. A finite element model was established to understand matrix deformation and interaction between tool-particle and further explain the tool wear phenomena observed. Additionally, cutting performance using AlTiN coated and uncoated was also investigated. The results indicated that the main wear mechanisms were identified as flank wear and edge chipping due to abrasive wear and chip adhesion in uncoated micro endmills. These wear mechanisms were confirmed by chip formation process produced by finite element modelling (FEM). It was also observed that the largest tool wear was occurred at smallest feed per tooth (0.75μm/tooth) and smallest wear was

occurred at largest feed per tooth (3µm/tooth). Also, the effect of BUE on tool wear and surface generation was studied.

Keywords: Micro milling; Tool wear; Metal matrix composites; Nanocomposite; Nanoparticles

# 1 Introduction

The demand for miniaturised components with complex features in micro scale has rapidly increased in many applications such as bioengineering, aerospace, medical and electronics in the last decade. Recently, a number of micro manufacturing technologies such as micro milling, micro electrical discharge machining, and micro laser machining have emerged to satisfy such demands. Micro milling is recognised as one of the most versatile micro manufacturing processes with high accuracy and machining capability of a wide range of engineering materials and hence has received considerable attention in the last decade [1]. In order to produce micro features, micro endmills ranging from 50-1000µm are typically used [1]. Although micro milling is kinematically similar to its conventional counterpart, a number of issues including size effect and minimum chip thickness arisen from the fact that uncut chip thickness is comparable with the cutting edge radius in micro milling [1]. These issues make the material removal mechanism in micro milling different from that in conventional milling. These down size related problems encountered with micro milling also limit its industrial applications.

Metal matrix composite materials have received considerable interests to replace conventional materials in various applications benefiting from their high specific strength, ductility, toughness and outstanding corrosion and fatigue resistance [2]. However, their superior mechanical properties, heterogeneous and anisotropic nature bring significant challenges in terms of premature and excessive tool wear and poor machined surface quality following machining processes. Therefore, the widespread applications of

conventional micro-sized reinforced MMCs are impeded due to their poor machinability caused by the reinforcement which is commonly harder than most of the commercial available tool materials [3, 4]. Li and Seah [5] conducted a comprehensive experimental study on tool wear mechanism during machining of Al/SiC MMCs using tungsten carbide tools. In this research, abrasive wear mode was found to be the main wear mechanism. Tool wear acceleration caused by interference between particles appeared when the weight fraction of particles reached a critical value. Pramanik et al. [6] created a finite element model to study the matrix deformation and interaction between tool-particle in orthogonal machining, and tool wear was found to be the result of the debonded particles sliding over the rake face and cutting edge leading to high localised stress during tool-particles interaction. Bhushan et al. [7] reported that a less severe tool wear was found in turning of conventional aluminium alloys compared with their composites using carbide and PCD inserts and abrasive wear was observed at the main wear mechanism. Ghani et al. [8] investigated milling and turning of AlSi/AlN MMCs using carbide cutting tools. Their results showed that a uniform flank wear caused by abrasion was the dominant wear mechanism. Although there are several research works on tool wear when machining MMCs with micro-sized particles, there are very limited publications on tool wear during micro machining of MMCs reinforced with nano-sized particles. Li et al. [9] reported that tool wear did not contribute to the variation of surface roughness in micro machining of SiC/Mg MMCs with nano-sized particles. Teng et al. [10] carried out an experimental investigation on micro milling of MMCs reinforced with nano-sized Ti and $TiB_2$ particles. Their results showed that chip adhesion effect which resulted in high cutting force and worse surface finish was more significant during machining of MMCs reinforced with Ti particles rather than that with $TiB_2$ particles. Additionally, the increase of volume fraction of reinforcement could lead to severe coating peeling off when coated tools were used.

The phenomena such as size effect and minimum chip thickness caused by scaling effects in micro milling

play an important role in material removal mechanism and underlying mechanics during machining process. The size of the ploughing region where the material elastically deforms and recovers to its original position after the tool pass cannot be neglected in micro milling. Consequently, it induces high friction and stress between the cutting tool and the materials which in turn makes the cutting edge the most loaded portion of micro endmills [11]. Therefore the unpredictable tool life and premature failure of micro endmills were recognised as the major barrier in micro milling [12]. Unlike in the conventional machining, wear mechanism in micro milling is diverse and complex. Additionally, tool wear measurement is challenging due to miniaturised size of endmills in micro milling. A literature survey shows that the current state-of-the-art lacks a generic tool wear criterion and assessment methods in micro milling. Some attempts in investigating tool wear mechanisms in micro milling of engineering materials are summarised below.

Tansel et al. [12] studied the wear mechanism of micro endmills when machining aluminium and mild steel and concluded that tool wear was mainly caused by fatigue and stress induced chip-clogging breakage. Another study carried out by Tansel et al. [13] established a relationship between tool wear and cutting force characteristic based on neural-network method in micro milling of aluminium and steel. A stable increase in cutting force with the progression of tool wear was observed. The latter caused an effectiveness/sharpness loss of cutting edge. Conversely, a sudden increase in cutting force before tool failure was reported in machining of steel. Rahman et al. [14] also investigated the effect of tool wear development on cutting forces where non-uniform wear and chip adhesion were observed on both major and minor cutting edges. This resulted in an increase of cutting forces and leads to an early tool failure. The abrasion wear which was found to be the dominant wear mode during micro milling of copper 101 using tungsten carbide tool was reported by Filiz et al. [15]. The stress acting on the cutting edge was found to dramatically increased when the material was elastically removed due to the size effect at low feed per

tooth. Therefore, greatest tool wear in the form of flank wear was experienced at low feed per tooth. The reduction of tool diameter was utilised as a measure of tool wear. Ucun et al. [16] compared the performance of endmills with different coatings during micro milling of Inconel 718 super alloy. The flank wear and cutting edge corner wear due to abrasive and chipping were reported as the dominant wear modes. Also, local fracture was observed due to the excessive friction on the part where smeared by workpiece material dominated by the size effect at small uncut chip thickness. Less chipping was observed in the coated tool which could be attributed to the extra toughness of the coating material when compared to the uncoated ones. Imran et al. [17] stated that the abrasion was initially experienced on TiN coated tool in wet drilling and followed by a cyclic workpiece adhesion on the cutting edge. Finally, the micro chipping which gradually increased the edge blunting was observed near the cutting edge due to the diffusion of workpiece materials into WC-Co binder with the assistance of adhesion effect. Overall, previous studies investigated tool wear mechanisms only based on the experimental method. Moreover, different wear mechanisms showed a diversity in machining different engineering materials but there are very limited publications available in investigating wear mechanism during machining MMCs with nano-sized particles.

This paper presents a comprehensive experimental investigation on the tool wear in micro milling of 1.98 Vol.% Mg/Ti MMCs under dry cutting condition. Tool wear was assessed by tool diameter reduction and flank wear. The wear mechanisms and effect of cutting parameters including feed per tooth and cutting speed on cutting force, surface roughness and burr formation was discussed by considering the size effect with the progression of tool wear. The performance of coated and uncoated cutting tool was compared. Both experimental and modelling techniques were employed in order to obtain a clear understanding of the wear mechanism.

## 2 Experimental methods

Magnesium turnings of 99.9% purity, supplied by ACROS Organics, New Jersey, USA were used as the base matrix. Reinforcement consist of pure titanium powder of 30-50 nm supplied by US Research Nanomaterials. Mg/Ti MMC was synthesized using the disintegrated melt deposition (DMD) technique. DMD process involved superheating the magnesium turning and the titanium powder reinforcement that were arranged in a multi-layered arrangement to 750°C in a graphite crucible under an inert argon atmosphere followed by stirring the molten melt at a speed of 465 rpm for 6 minutes using a twin blade (pitch 45°) mild steel impeller coated with Zirtex-25. The melt is then released from the base of the crucible, disintegrated by two jets of argon orientated normal to the melt stream and deposited onto a metallic substrate. The preforms were machined to remove the outer layer and cut into small billets. The billets are soaked in a constant temperature furnace at 400°C for 1 hour before being hot extruded at 350°C using an extrusion ratio of 20.25:1 on a 150 tonne hydraulic press to obtain 8mm diameter rods which were used for characterization studies. Further details of the DMD processing technique have been described elsewhere [insert new ref 2 and ref 18 by Ganesh]. The distribution of nano Ti particles within Mg/Ti MMCs was observed through Scanning electron microscope (SEM) in Figure 1.

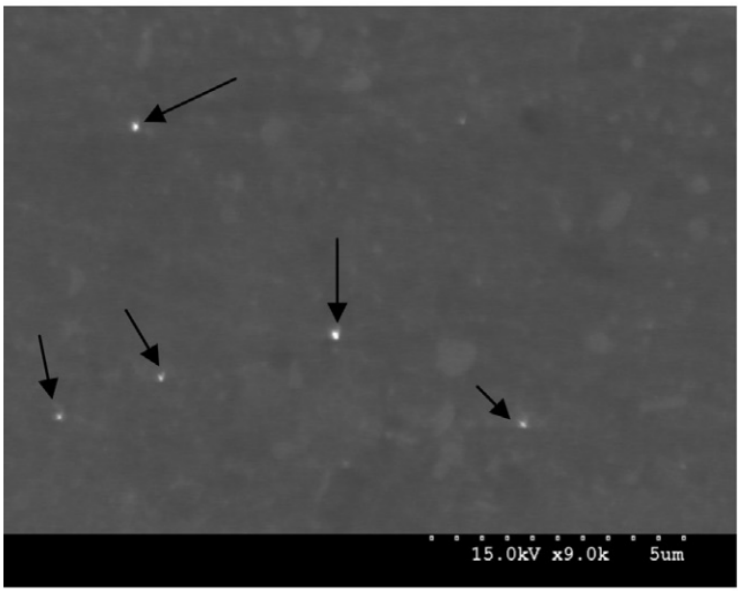


Figure 1. Distribution of nano Ti particles in Mg/Ti MMCs [18]

Two flutes uncoated and AlTiN coated micro-grain tungsten carbide endmills with nominal cutting diameter (D) of $0.5^{+0.00mm}_{-0.02mm}$ mm and helix angle of 20° were used. The dimension and geometry of the micro endmill are illustrated in Figure 2, 4 & 5. The cutting edge radius of new tools was measured using SEM and was estimated to be 2.0 µm in average (Figure 4(b)). As the flank wear and reduction in effective tool diameter affect the machining accuracy and surface integrity, the effective tool diameter $D_E$ and average flank wear $V_{BA}$ were used as tool wear criteria and measured as shown in Figure 3. Flank wear $V_B$ is defined as the band width in a direction perpendicular to the original cutting edge where the grinding marks from manufacturing process were removed by abrasive and chipping worn marks on the flank face of endmill. The measurement of flank wear was carried out at four consistent positions at different endmill and an average value, $V_{BA,}$ was computed. All endmills were selected from the same batch to eliminate the effect of tool manufacturing errors.

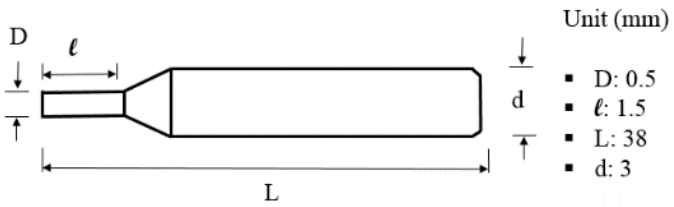


Figure 2. Dimension of the micro endmill (uncoated & coated)

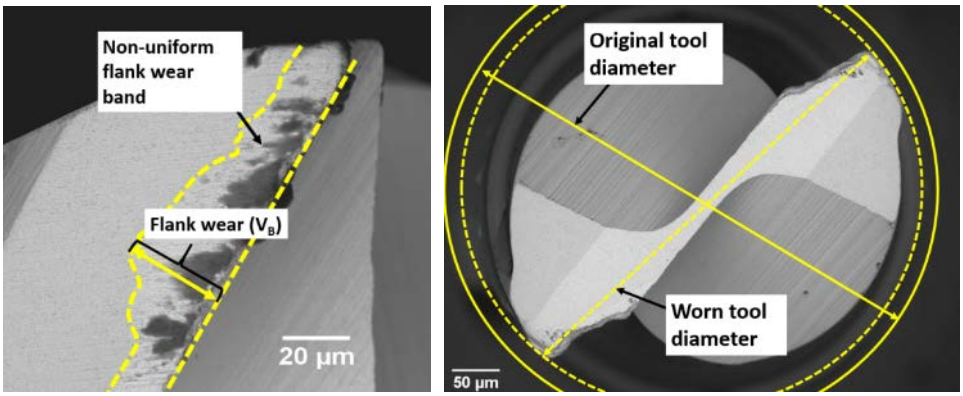


Figure 3. Measurement of (a) flank wear, $V_B$ and (b) effective tool diameter ($D_E$)

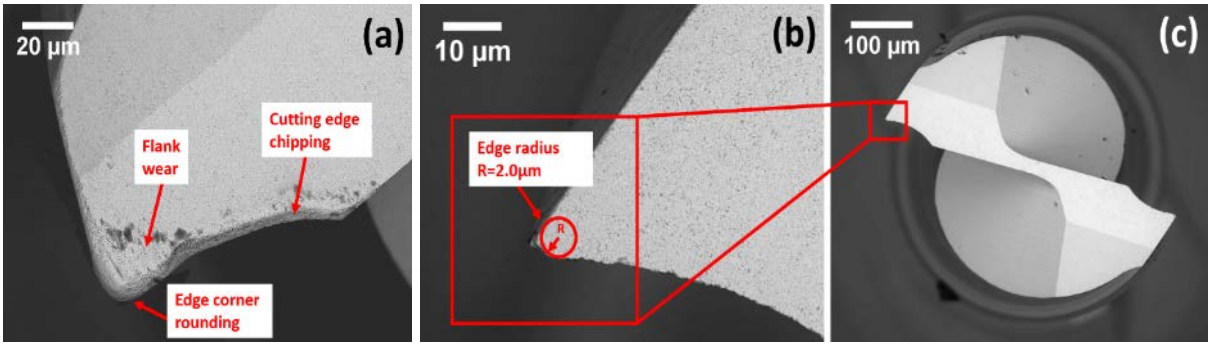


**Figure 4.** Top view of SEM micrograph for (a) worn tool (Tool #1), (b) & (c) new tool (uncoated endmill).

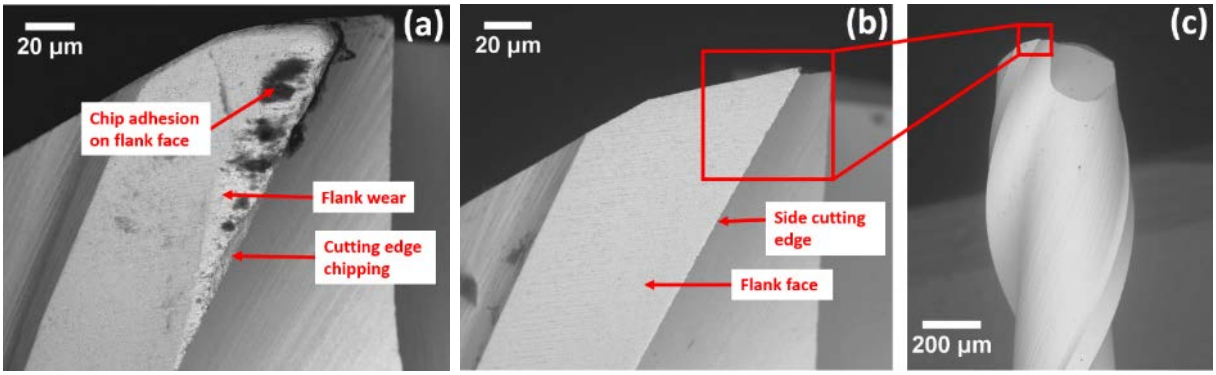


**Figure 5.** Side view of SEM micrograph for (a) worn tool (Tool #1), (b) & (c) new tool (uncoated endmill).

Magnesium based metal matrix composites (Mg/Ti MMCs) reinforced with 1.98 Vol.% nano-sized titanium

particles (approx. 30-50 nm) was used as workpiece throughout the research. The lightweight Mg-Ti nanocomposites has higher specific mechanical strength when compared to pure magnesium. Metallic reinforcements such as titanium with superior mechanical properties was found to produce an acceptable compromise in ductility compared to the addition of ceramic reinforcements SiC, $Al_2O_3$ and TiC MMCs. The mechanical properties of Mg/Ti MMCs are shown in Table 1.

**Table 1** Mechanical properties of 1.98 Vol.% Mg/Ti MMCs

| **Density (g/cm3)** | **0.2 Yield Strength (MPa)** | **Ultimate tensile strength (MPa)** | **Ductility (%)** | **Microhardness (HV)** | **Grain size (μm)** |
|---|---|---|---|---|---|
| 1.793 | 162 ± 5 | 231 ± 12 | 7.7 ±0.1 | 70±2 | 1.25 ± 0.25 |

Micro milling experiments were undertaken on an ultra-precision desktop micro-machine tool (Nanowave MTS5R) equipped with a high speed spindle (max 80,000rpm). The spindle runout was measured to be less than 2 μm. Total volume of 620 $mm^3$ of workpiece material was removed in each set of experiment. 6 sets of machining experiments and the cutting parameters for each set of experiment are detailed in Table 2. Brand new tools were measured before performing each set of experiments. Full-immersion slot milling with a constant axial depth of cut of 100 μm was employed in all experiments. For each set of experiment, a total volume of 620 $mm^3$ of workpiece material was removed at 4 even intervals, i.e. a volume of 155$mm^3$ of workpiece materials in each interval. The tools were then measured after each interval. The cutting forces along the X, Y and Z axis was measured using a Kistler piezoelectric dynamometer (9256C2). A scanning electron microscope (SEM, Hitachi TM3030) was used to acquire the micrographs of the worn tools. A white light interferometer (Zygo NewView 5020) was employed to measure surface roughness of the machined slot.

**Table 2** Cutting parameters for each set of experiment

| **Exp set/Tool #** | **Cutting speed, $Vc$ (m/min)** | **feed per tooth, $f_z$(μm/tooth)** | **Tool** |
|---|---|---|---|

| | | | |
|---|---|---|---|
| **1** | 31.4 | 3 | uncoated |
| **2** | 62.8 | 3 | uncoated |
| **3** | 125.6 | 3 | uncoated |
| **4** | 62.8 | 0.75 | uncoated |
| **5** | 62.8 | 1.5 | uncoated |
| **6** | 62.8 | 3 | AlTiN-coated |

# 3 Results and discussion

## 3.1 Tool wear mechanism analysis

A better understanding of tool wear benefits from observing highly magnified SEM micrographs of the endmills. A significant reduction in the effective tool diameter is observed (an example is shown in Figure 3(b)) due to the decrease of cutting edge radius. All endmills used in this experiment exhibited similar wear behaviour. A significant amount of volume loss of tool material is found in the main cutting edge in all tools used in this experiment. A comparison between the new tool and worn tool (Tool #1) on the side and top view is illustrated in Figure 4 and Figure 5. Figure 6 shows the progression of tool wear against different cutting conditions. It is noted that a significant amount of tool wear with the combination of non-uniform flank wear and cutting edge chipping is found on the side cutting edge and flank face of all five uncoated endmills. For the AlTiN coated tools, delamination and flank wear were the dominant wear mechanism.

### 3.1.1 Effect of cutting speed

Figure 7 illustrates the effect of cutting speed on flank wear and reduction in tool diameter with the increasing cutting volume at constant depth of cut and feed per tooth. Understandably, flank wear and reduction in tool diameter increases with cutting volume under all cutting parameters. As shown in Figure 8(a), the largest wear was experienced at cutting speed of 31.4 m/min. The largest trend on the progression of flank wear was observed at the cutting speed of 62.8 m/min, namely, this cutting speed produces the

smallest wear after cutting volume of 155 $mm^3$ and largest wear after cutting volume of 620 $mm^3$ compared with other cutting speed. In addition, the flank wear obtained at 125.6 m/min provided the most stable trend and the smallest flank wear after cutting volume of 620 $mm^3$ was measured. The smallest tool diameter reduction is obtained at the largest cutting speed of 125.6m/min (Figure 7(b)), which is consistent with the trend in flank wear.

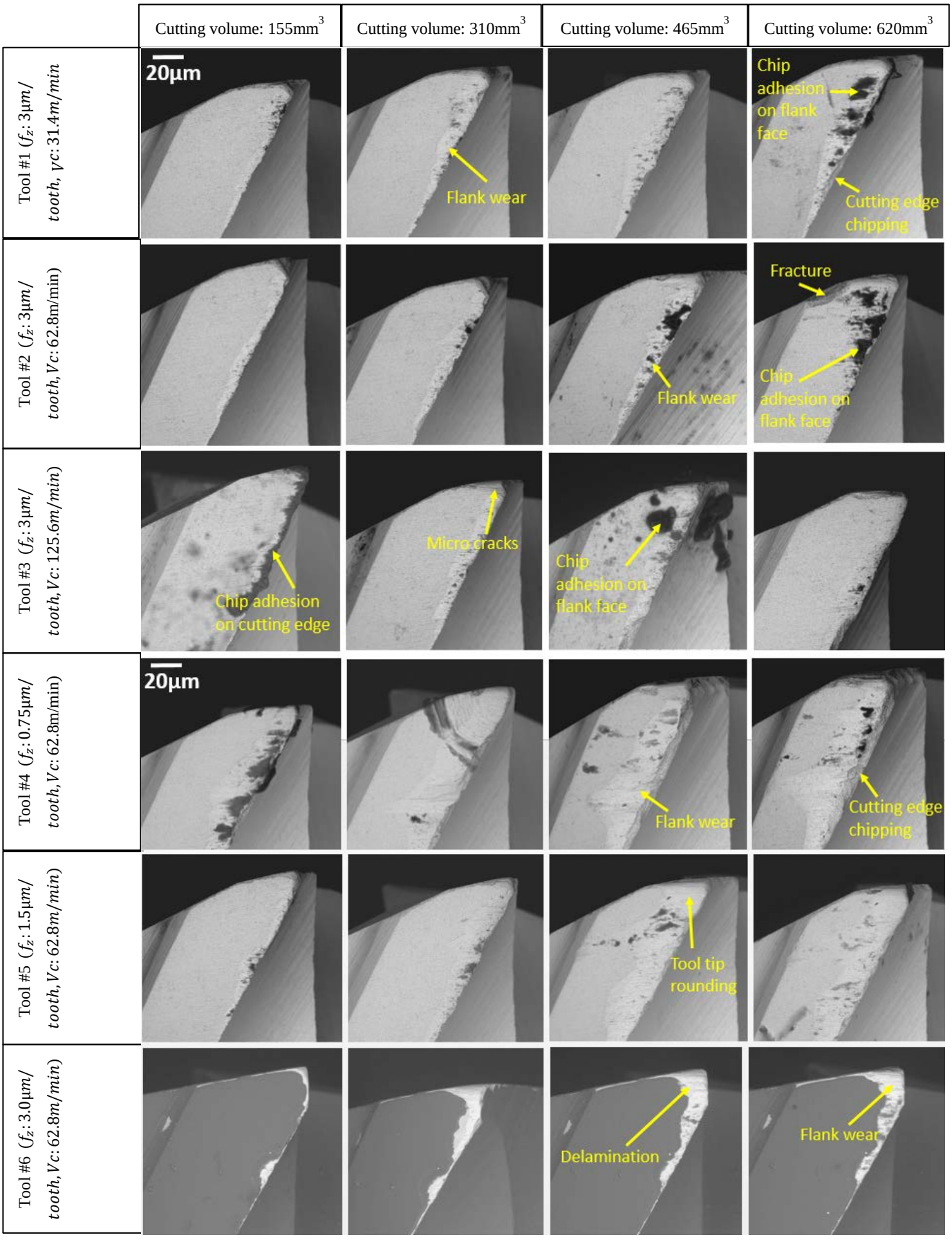


**Figure 6.**SEM micrographs of the tool wear progression under various cutting conditions

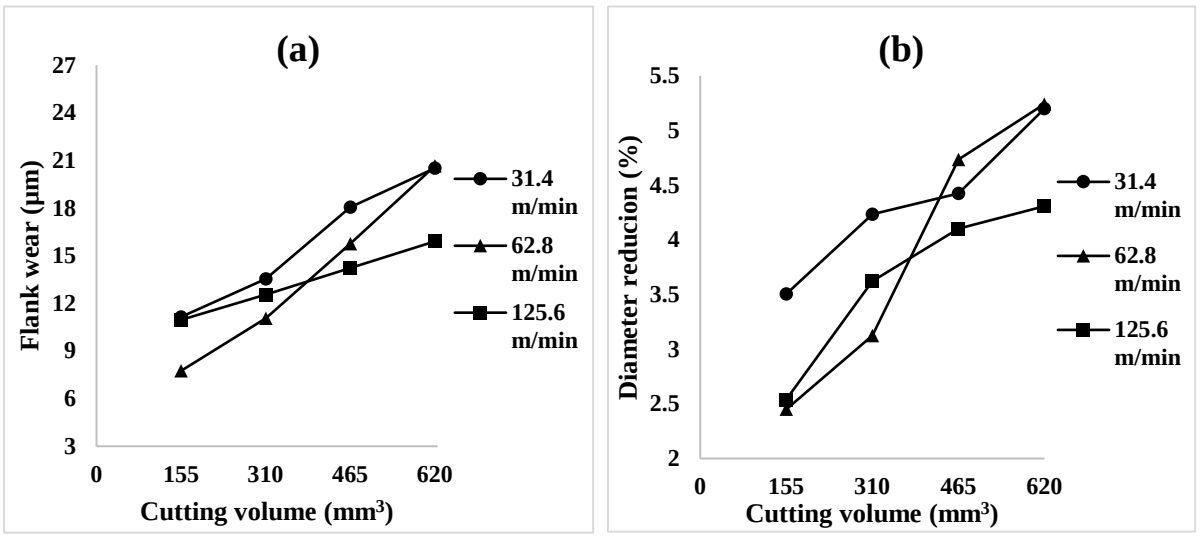


**Figure 7.** The effect of cutting speed on the progression of (a) flank wear; (b) reduction in tool diameter at constant feed per tooth of 3µm/tooth and depth of cut of 100 µm.

Figure 8 and 9 illustrate the SEM micrographs and EDS spectra of the uncoated endmills after cutting volume of 620 $mm^3$ of the workpiece material and at a constant feed per tooth of 3µm/tooth, depth of cut of 100 µm with cutting speed of 31.4m/min, 62.8m/min and 125.6m/min. Extensive abrasive marks and chipping wear along the flank face and cutting edges are observed from cutting speed of 31.4 and 62.8 m/min (Figure 8 (a & b)). In addition, the chip adhesion was observed on the flank face of Tool #1 and Tool #2 (Figure 8 (a & b)). The EDS spectra performed on flank face (Figure.8 (c & d)) shows the presence of excessive element of magnesium (Mg), and titanium (Ti). Chip adhesion can cause high friction during the interaction between the flank face and workpiece which is more evident in elastic dominated machining process. Additionally, the existence of titanium element on flank face from EDS spectra would confirm the abrasive effect contributed by hard reinforced particles. Based on this assumption, it is thought that local stressing would be induced on the cutting edge and flank face, which is a consequence of the hard reinforcement abrading through the cutting edge especially during elastic dominated cutting zone. Conversely, it can be seen from the EDS spectra obtained from the flank face (Figure 9(b)) that the chip adhesion effect is not evident and tool wear is considerably reduced at the cutting speed of 125.6m/min.

Small amount of flank wear with only partial chipping is observed at cutting edge, which indicates that the gradual abrasive wear dominates the cutting process. At the initial cutting stage, small amount of built-up edge (BUE) is found after cutting volume of 155 $mm^3$ at cutting speed of 125.6m/min and feed per tooth of 3µm/tooth (Tool #3 at Figure 6). This is believed to be the main reason to protect the cutting tool from chipping and flank wear. The friction condition at the tool-material interface is affected by the built-up edge that acts as a protecting layer preventing the cutting edge being in contact with workpiece during machining process [19].

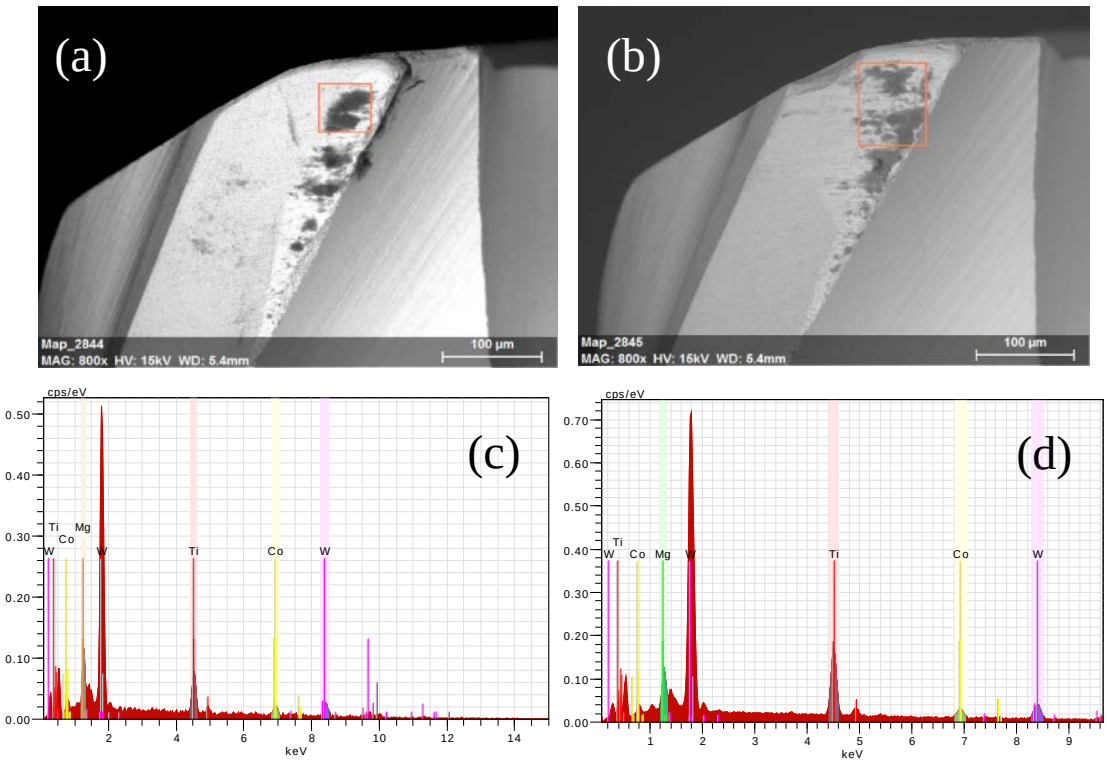


**Figure 8.** SEM micrographs and EDS spectra of uncoated endmills after cutting volume of 620 $mm^3$ from (a)(c) Tool #1 (cutting speed of 31.4m/min), (b)(d) Tool #2 (cutting speed of 62.8m/min) at feed per tooth of 3µm/tooth and depth of cut of 100 µm (with adhesion effect).

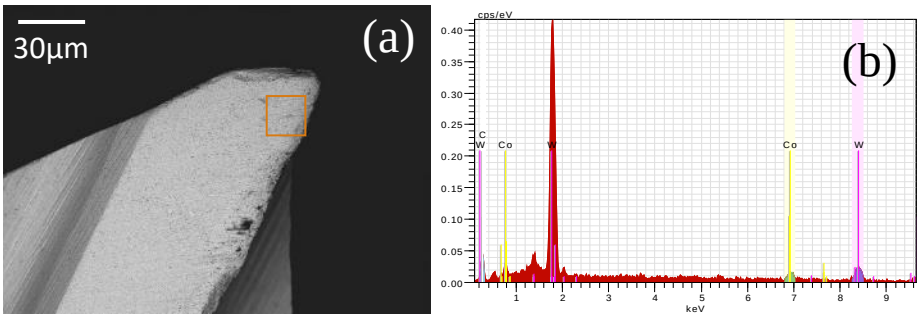


**Figure 9.** SEM micrographs and EDS spectra of uncoated endmill after cutting volume of 620 $mm^3$ from Tool #3 (cutting speed of 125.6 m/min) at feed per tooth of 3µm/tooth and depth of cut of 100 µm (without adhesion effect).

With regards to the effect of cutting speed on the average cutting force, Figure 15(a) reveals a stable increase in the average cutting force with the smallest increasing rate at 125.6m/min compared with that obtained from 31.4 m/min and 62.8m/min. This trend can be reasonably associated with the accumulation of material in front of the cutting edge which prevents it from edge chipping and rounding. This can be confirmed by the fact that cutting tool diameter obtained at 125.6m/min exhibits the smallest reduction compared with other cutting speeds due to the abrasive and chipping wear on the cutting edge which were the main reason causing the reduction in effective tool diameter.

### 3.1.2 Effect of feed per tooth

According to the observation on the effect of feed per tooth on the tool wear (Figure 10), it can be seen that flank wear and reduction in tool diameter increases with the decrease of feed per tooth. The largest wear was recorded at the smallest feed per tooth of 0.75µm/tooth while the largest feed per tooth of 3µm/tooth resulted in the smallest wear. This is in line with the results from [18]. SEM micrographs of the severely worn endmill (Tool #4) is shown in Figure 6. The most severe flank wear with edge chipping was found after cutting volume of 620 $mm^3$. Based on the observation of EDS spectra (Figure 11), chip adhesion was not evident and an increasing volume loss of tool material was observed on the cutting edge and edge corner leading to the most severe wear in all experiments. This can be attributed to the cutting edge radius size effect. The instantaneous uncut chip thickness varies during each tool pass in slot milling. The uncut chip

thickness starts from zero at the initial contact with the workpiece, followed by an increase to its maximum value as the tool rotates ninety degree, and then decrease to zero when cutting edge leaves workpiece. As a result, the ploughing region in each tool passing cycle at small feed per tooth is larger when compared with that at larger feed per tooth and the ploughing effect could dominate the cutting process when the uncut chip thickness is close to the minimum chip thickness. The ploughing effect could cause a significant portion of materials to be rubbed underneath the cutting edge and elastically deformed, and the workpiece material recovers to its original position without proper chip formation after the cutting edge passes, which induces a higher cutting force. Therefore, the abrasive wear mechanism resulting in a large flank wear and edge chipping is induced at small feed per tooth of 0.75μm. This can be contributed to the high frictional and normal stress experienced by cutting edge which exceeds the strength of the tool materials during each tool passing [20]. Additionally, unlike turning process, the intermittent material removal mode and instantaneous changing uncut chip thickness in micro milling produce high frequency shocking loads to cutting edges and hence results in the edge chipping. This is believed to be another important contributing factor to higher tool wear rate. At higher feed per tooth, shear mode dominates most of the cutting process which leads to a uniform distributed stress on the cutting edge, resulting in a reduced tool wear rate.

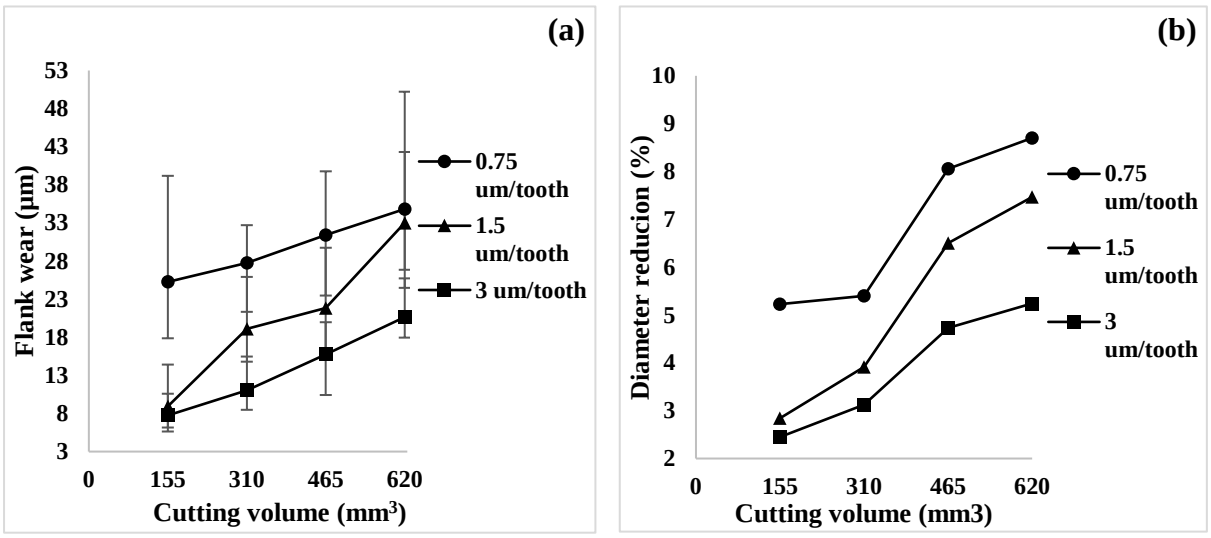


**Figure 10.** The effect of feed per tooth on the progression of (a) flank wear; (b) reduction in tool diameter at constant cutting speed of 62.8 m/min and depth of cut of 100 µm.

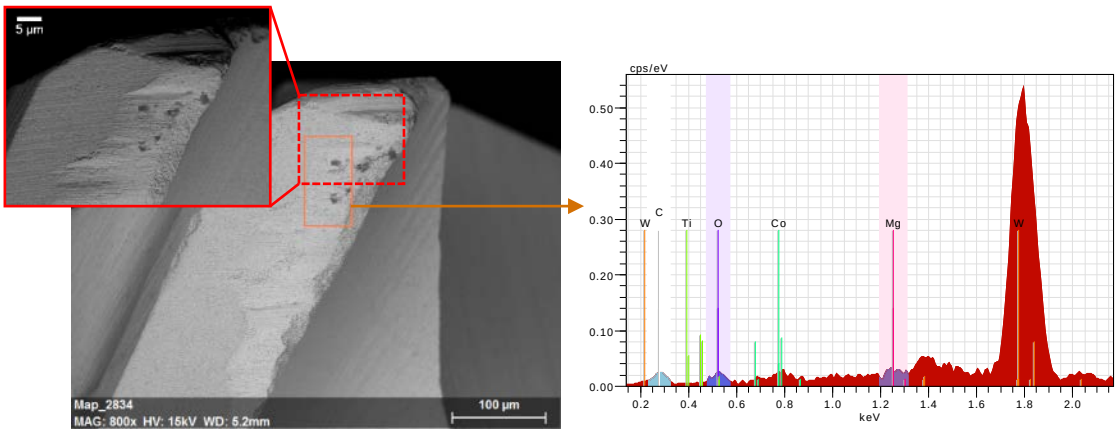


**Figure 11.** SEM micrographs and EDS spectra of uncoated endmill after cutting volume of 620 mm$^3$ from Tool #4 (feed per tooth of 0.75µm/tooth) at cutting speed of 62.8 m/min and depth of cut of 100 µm.

### 3.1.3 Effect of tool coating

Delamination was identified as the principal wear mechanism on the coated tools. Chip adhesion and built-up edge are not observed on the coated tool. It can be noticed that the AlTiN coating showed a better resistance to the chip accumulation under the cutting conditions used in this study. Figure 12 compares the performance of coated and uncoated tool in terms of reduction in tool diameter. A faster reduction rate was observed at the uncoated tool resulting in a higher value after cutting volume of 620 mm$^3$ comparing with coated tool. Figure 13(a) shows SEM micrograph of the AlTiN coated tool after cutting volume of 620 mm$^3$.

A complete coating delamination was found along the flank face and cutting edge with the effect of machining stress. However, cutting edge was found intact without chipping which indicates a gradual abrasive wear. Additionally, a large presence of tungsten which is the main element of tool material was found on EDS spectra obtained from the area marked in Figure 13(a). The abrasive wear caused by hard titanium particles and the poor adhesion between the coating materials and the tool base substrate likely contributed to the coating delamination.

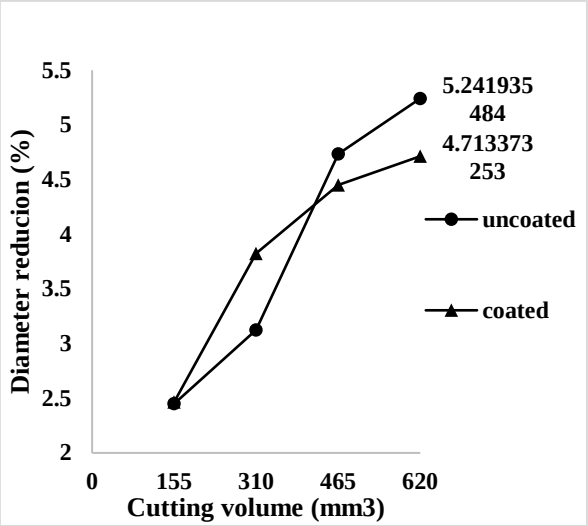


**Figure 12.** The effect of tool coating on the progression of reduction in tool diameter at constant feed per tooth of 3µm/tooth, cutting speed of 62.8 m/min and depth of cut of 100 µm.

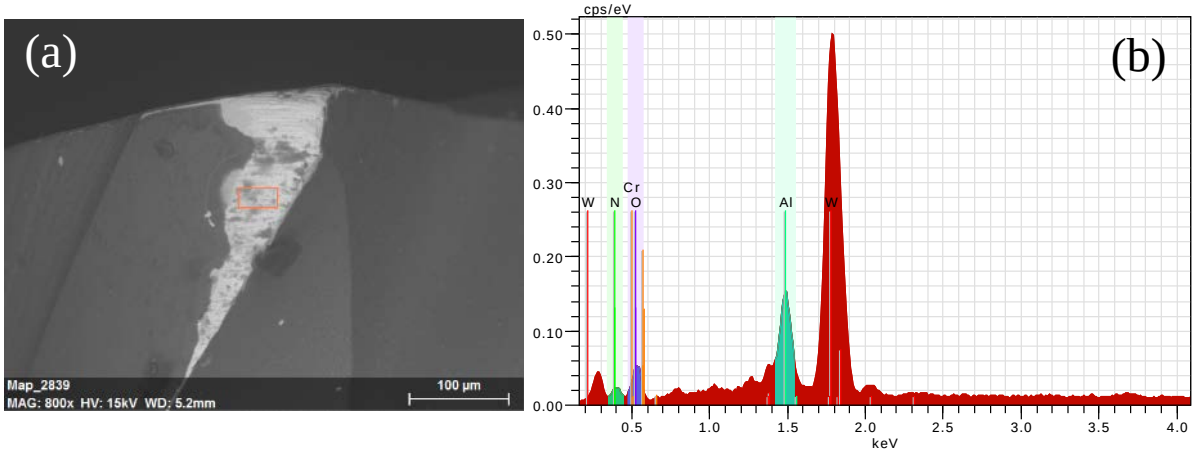


**Figure 13.** SEM micrographs and EDS spectra of coated endmill after cutting volume of 620 $mm^3$ from Tool#6 at constant feed per tooth of 3µm/tooth, cutting speed of 62.8 m/min and depth of cut of 100 µm.

### 3.1.4 Simulated interaction between nanoparticle and cutting tool

To further investigate the chip formation process and interaction between the particles and cutting edge, a heterogeneous two-dimensional finite element model (FEM) was established to simulate micro scale orthogonal cutting of magnesium based MMCs reinforced with nanosized SiC particles using ABAQUS/Explicit. It can be seen from Figure 14(a) that an irregular shear zone was formed in front of the rake face and cutting edge with stress magnitude of 470 MPa at initial engagement. As the tool moves (Figure 14(b)), the material was rubbed by cutting edge and a crack is initiated near the shear zone. As the cutting progresses, a crack was completely formed resulting in a segmented chip formation. In addition, the largest von Mises stress of 943.5 MPa observed at the particle was embedded within the chip root and came in contact with the cutting edge (Figure 14(c)). This confirms the assumption that high local stress induced on the cutting edge resulted in the abrasive effect. The above-mentioned process repeats after the formation of segmented chips (Figure 14(d)). A high von Mises stress was then induced near the flank face as the tool fully engaged with the workpiece. This can be the evidence of high friction induced on the flank face due to the effect of chip adhesion.

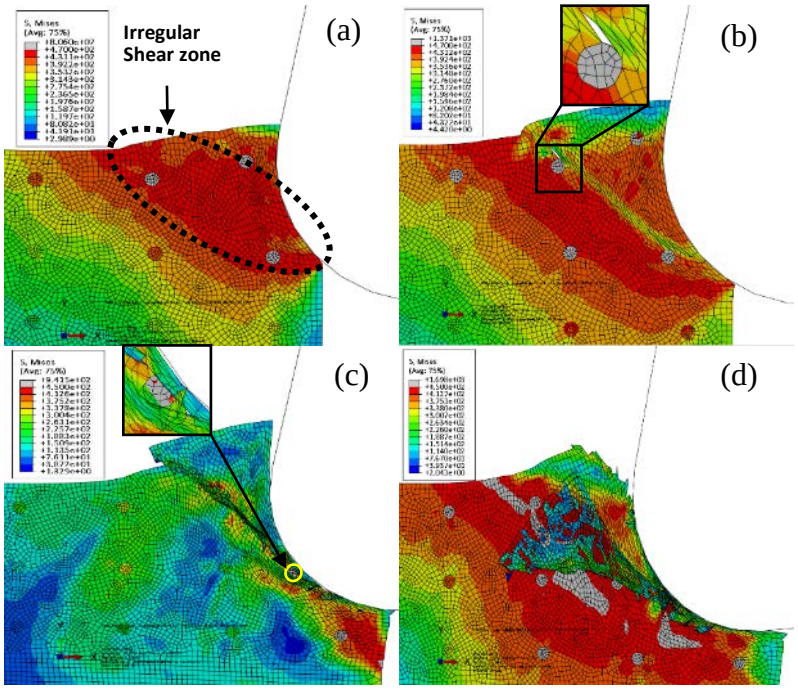


**Figure 14.** Chip formation process of micro orthogonal machining of MMCs with nano-particles

## 3.2 Cutting force

To gain a better understanding of the effect of tool wear on the machinability, an average cutting force was calculated by collecting the peak-to-valley forces for each revolution and 500 revolutions was collected in total. Figure 15 presents the variation of average cutting force with the progression of tool wear under various cutting speed, feed per tooth and tool coating. The cutting force obtained from new tool was also captured (labelled at volume of 0 $mm^3$). It can be seen from Figure 15 (a) that the largest cutting force is experienced at cutting speed of 31.4m/min after cutting volume of 620 $mm^3$ although this cutting condition can produce the smallest tool wear in terms of flank wear and diameter reduction. A stable increase in the cutting force was observed from cutting volume 0 to 620 $mm^3$ at the cutting speed of 125.6m/min that corresponds to the variation of flank wear.

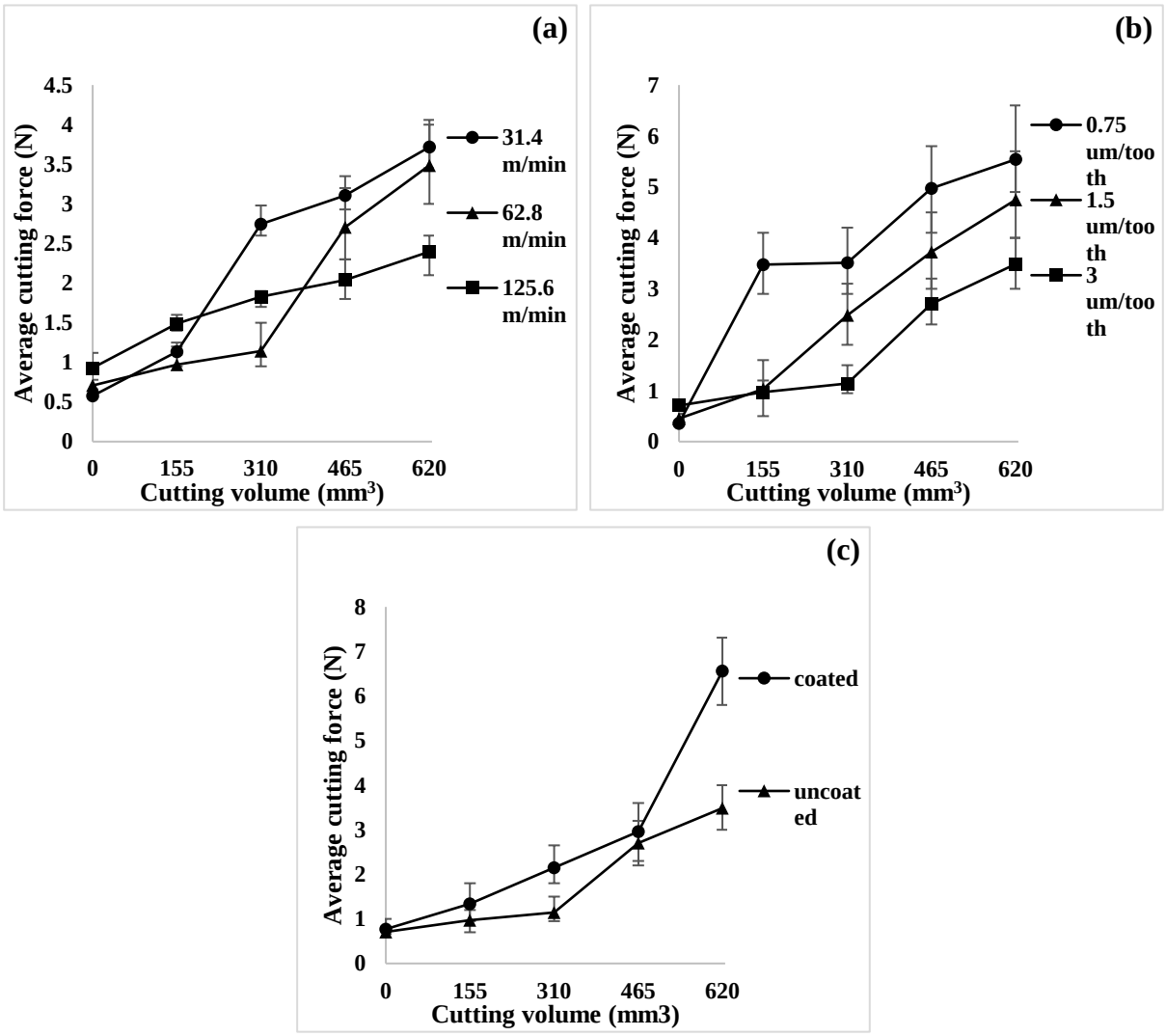


**Figure 15.** Variation of average cutting force with progression of tool wear under the effected by (a) cutting speed at feed per tooth of 3µm/tooth and depth of cut of 100 µm; (b) feed per tooth at cutting speed of 62.8 m/min and depth of cut of 100 µm; (c)tool coating

With regard to the influence of size effect on the tool wear, Figure 15 (b) shows the effect of feed per tooth ranging from 0.75 to 3 µm/tooth (cover the minimum chip thickness) on the cutting force. It can be noted that the smallest feed per tooth of 0.75µm/tooth produced the largest cutting force, which can be considered as the main reason to cause the largest tool wear. Also, a sudden increase in the cutting force was seen from cutting volume 0 to 155 $mm^3$, which was correlated to the observation where significant flank wear and chipping on endmill after cutting volume of 155 $mm^3$ (Tool #4, Figure 6) compared to other experiments. To further confirm the significant role played by size effect on the tool wear, Figure 16 compares the

variation of flank wear and specific cutting force with the effect of feed per tooth. The specific cutting force can be defined as the chip load required to remove a unit volume of material and it was calculated by dividing the cutting force by the section area of chips. As illustrated in Figure 16, highest specific cutting force was experienced at lowest feed per tooth, while the specific cutting force at each feed per tooth increases with the flank wear. In addition, nearly 5 times larger of the specific cutting force (72.8 J/mm$^3$) at feed per tooth of 0.75µm/tooth can be found than that at 3 µm/tooth (18.25 J/mm$^3$) after cutting volume of 620 mm$^3$. By considering this information, it can be thought that the ratio of cutting edge radius to uncut chip thickness increases so that the material removal mechanism dominated by elastic deformation is becoming evident with the progression of flank wear.

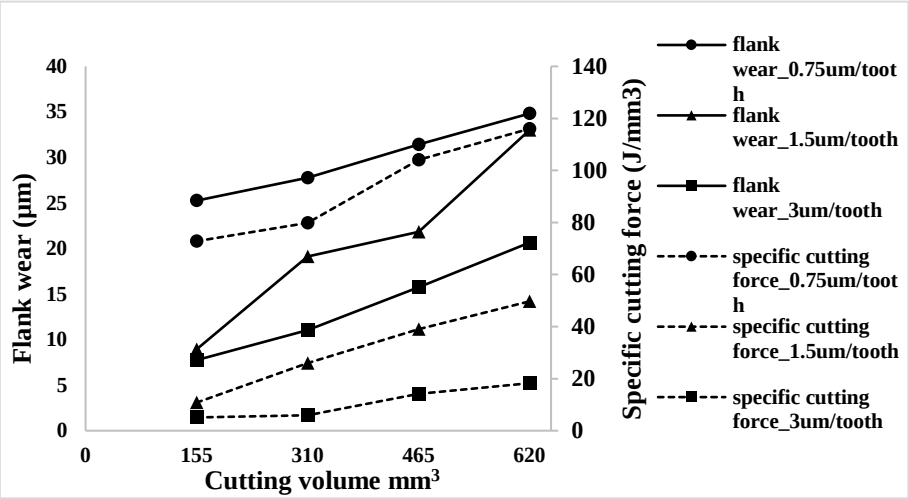


**Figure 16.**The comparison between the flank wear and specific cutting force with the effect of feed per tooth at the cutting speed of 62.8m/min, depth of cut of 100µm.

For the effect of tool coating on the cutting force, it is interesting to note from Figure 15 (c) that the cutting force obtained from coated tool exhibits higher values from cutting volume 155 to 620 mm$^3$ than that from uncoated tool. This can be correlated with the delamination effect induced at the initial stage of cutting (cutting volume of 155 mm$^3$) which increases the cutting edge radius.

## 3.3 Surface roughness & burr formation

In order to clearly understand the relationship between the tool wear and surface quality, average surface roughness Ra was measured for all samples (Figure 17). It can be seen from Figure 17(a) that at the constant depth of cut of 100µm with a feed of 3 µm/tooth, cutting speed of 62.8m/min generates the lowest surface roughness. In contrast, the surface roughness obtained at 125.6m/min is the highest. As known that the deterioration can be induced on the surface roughness due to existence of BUE under certain machining conditions. This might be contributed to the adhesion effect of the BUE (Figure 19) on the machined surface. Some loose portion of BUE is thought to be adhered to the bottom surface of micro channels, which results in a deteriorated surface roughness. As expected, the highest surface roughness is obtained by the tool with large wear at smallest feed (0.75 µm/tooth). At this feed rate, the material is removed by relatively large cutting edge radius causing severe edge chipping (Figure 18). This indicates that the surface generation mechanism is dominated by ploughing and elastic deformation effect. The surface roughness decreases with increasing feed per tooth. This confirms the fact that the shearing mechanism becomes more dominant at larger feed rate. The results show a good agreement with the wear measurement. With regards to the effect of tool coating on surface roughness at Figure.17 (c), minor variation was observed in surface roughness results which indicate that coating has limited impact on surface quality.

To qualitatively compare burr formation at different cutting conditions and correlate its size with tool wear progression, SEM micrographs of the top burr at various cutting volumes were obtained (Figure 20). It can be seen that the burr formation is strongly dependent on tool wear conditions especially in the down milling side Figure 20 (a- d). At the feed rate of 3µm/tooth (Figure 20(a-c)), an increased size of the top burrs was observed with the increase of tool wear. Additionally, cutting speed of 125.6m/min (Figure 20 (c)) generates the slots with the smallest burr size, which corresponds to the smallest tool wear obtained at these cutting

conditions. At the cutting speed of 62.8m/min (Figure 20 b, e, d), the rise of feed per tooth from 0.75 to 3 µm/tooth results in a reduced burr size. The largest burrs formation is obtained at smallest feed per tooth of 0.75 µm Figure 20 (d).

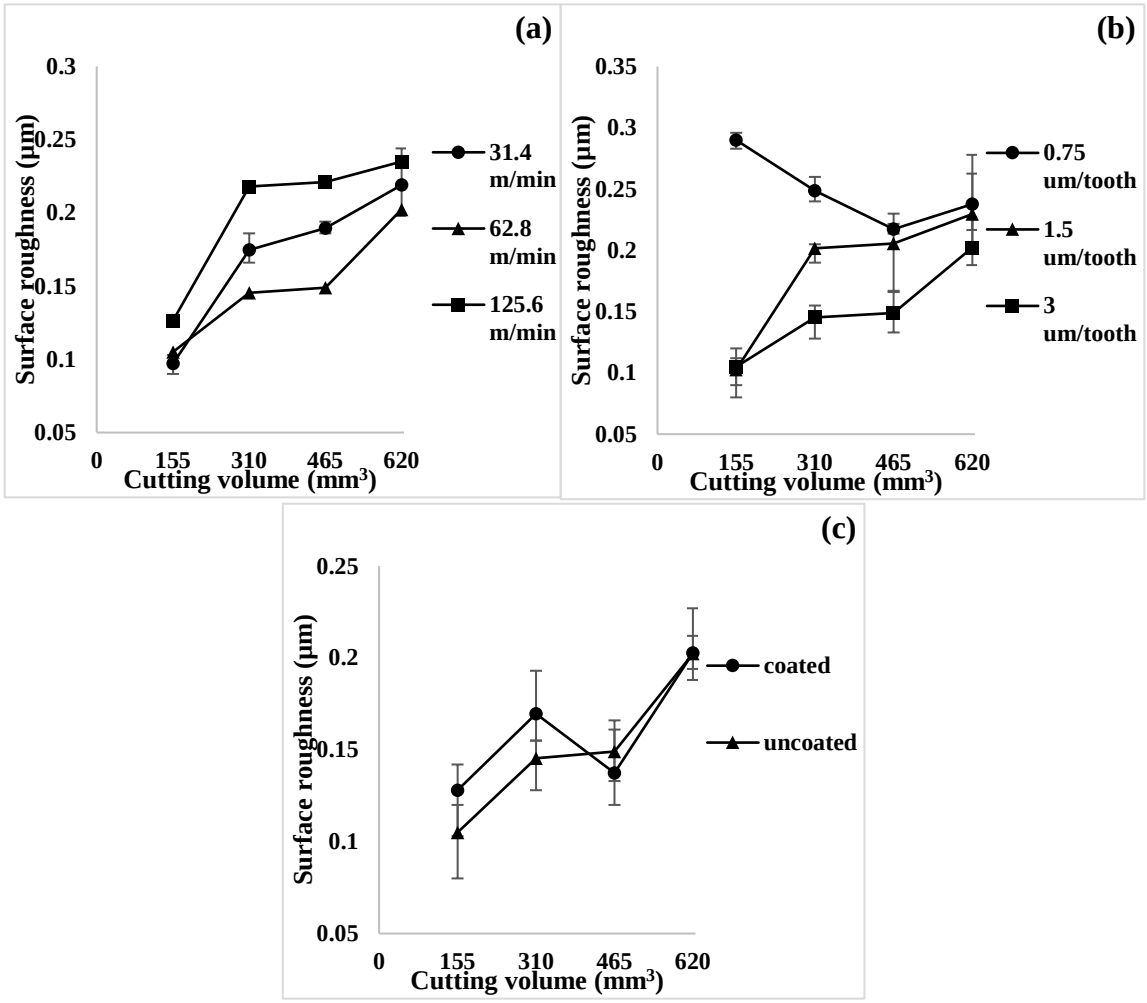


**Figure 17.** Surface roughness under effected by (a) cutting speed at feed per tooth of 3µm/tooth and depth of cut of 100 µm; (b) feed per tooth at cutting speed of 62.8 m/min and depth of cut of 100 µm; (c) tool coating at feed per feed per tooth of 3µm/tooth, cutting speed of 62.8m/min and depth of cut of 100 µm.

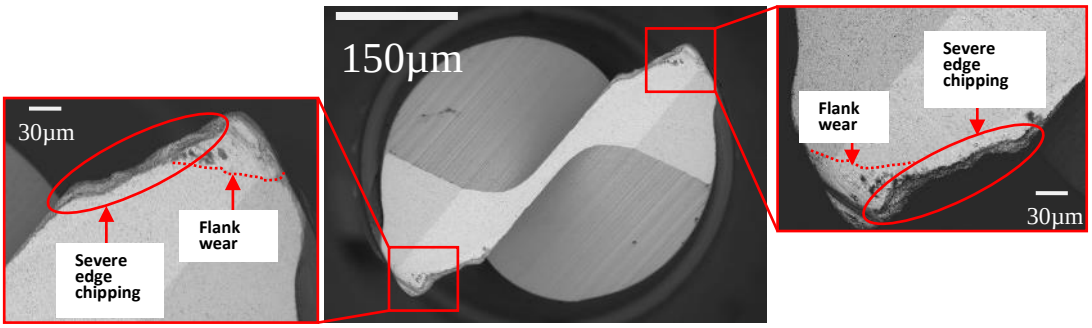


**Figure 18.** Top view of worn endmill obtained at Tool #4 (cutting speed of 62.8m/min, feed per tooth of 0.75 µm and depth of cut of 100 µm)

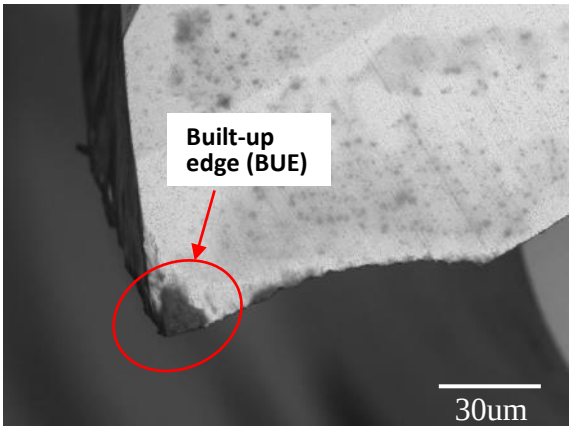


**Figure 19.** Built-up edge formed on cutting edge corner at Tool #3 (cutting speed of 125.6m/min, feed per tooth of 3 µm and depth of cut of 100 µm)

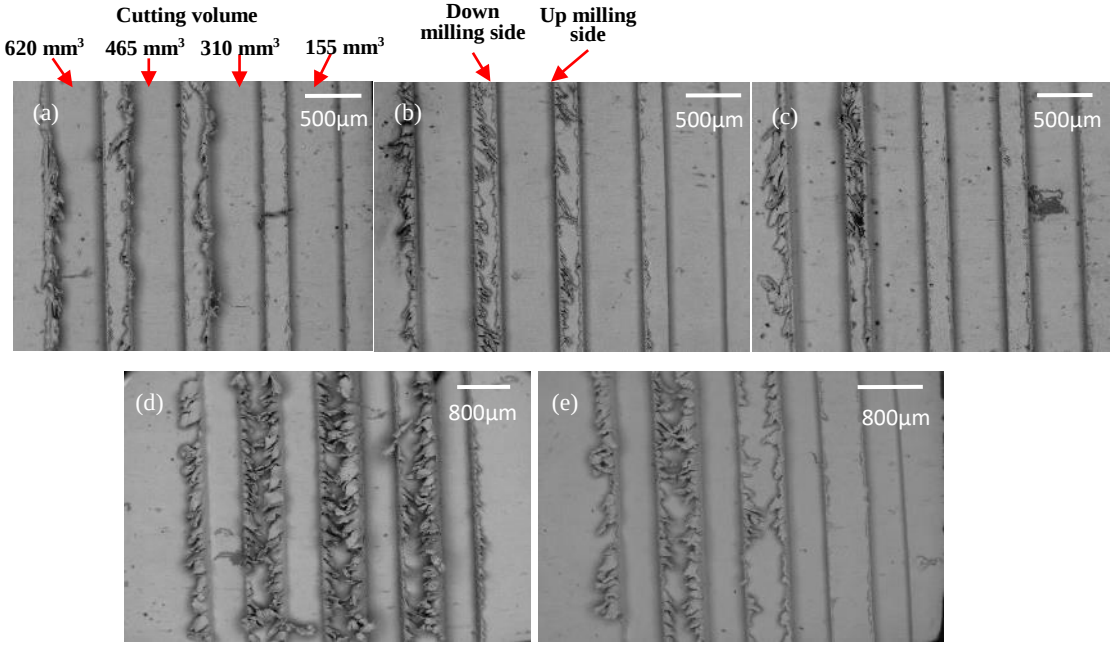


**Figure 20.** Burr formation at varying Experiment: (a)Experiment.1, cutting speed of 31.4m/min, feed per tooth of 3µm/tooth; (b) Experiment 2, cutting speed of 62.8m/min, feed per tooth of 3µm/tooth; (c) Experiment 3, cutting speed of 125.6m/min, feed per tooth of 3µm/tooth; (d) Experiment 4, cutting speed of 62.8m/min, feed per tooth of 0.75µm/tooth; (e) Experiment 5, cutting speed of 62.8m/min, feed per tooth of 1.5µm/tooth at constant depth of cut of 100 µm.

## 4. Conclusions

This paper presents a comprehensive experimental investigation on the effect of cutting parameters and tool condition on the progression of tool wear in terms of flank wear and reduction in tool diameter when micro milling of 1.98 Vol.% Mg/Ti MMCs. The relation between tool wear and the cutting force, surface roughness and burr size was also investigated. Moreover, tool wear behaviour for uncoated and coated tools was compared. The following conclusions can be drawn:

- Flank wear and edge chipping due to abrasive wear and chip adhesion were observed as the main wear mechanisms during all cutting conditions for uncoated endmills. This has been confirmed by

the chip formation process established using finite element modelling (FEM)

- The largest tool wear was generated at the lowest feed per tooth of 0.75μm/tooth whereas the smallest wear was experienced at the highest feed of 3 μm/tooth. Meanwhile, the highest average cutting force and surface roughness were obtained at the highest tool wear. This phenomenon was attributed to the elastically dominated materials removal mechanism in small feed, namely, size effect.
- At 3 μm/tooth feed per tooth and depth of cut of 100 μm, built-up edge (BUE) was found at the cutting edge in particular at the cutting speed of 125.6m/min. And a smaller tool wear along with the highest surface roughness was observed when compared to that at 62.8m/min and 31.4m/min. This can be explained by the existence of BUE.
- A faster reduction rate was observed at the uncoated tool resulting a higher value after cutting volume of 620 $mm^3$ comparing with coated tool. Abrasive wear mechanism and poor adhesion of coating to the tool substrate were considered as the main reasons for coating delamination which was found to be the main wear mode. Chip adhesion was not observed on all cutting tools.

## Acknowledgement

The authors wish to thank the Engineering and Physical Sciences Research Council (EP/M020657/1) and the Visiting Scholar Foundation of the State Key Lab of Mechanical Transmission in Chongqing University (SKLMT-KFKT-201613) for the support.

## References

1. Cheng K, Huo D (2013) Micro Cutting: Fundamentals and Applications. John Wiley & Sons Ltd, Chichester, UK
2. Gupta WM, Wong WLE (2015) Magnesium-Based Nanocomposites: Lightweight Materials of the Future. Materials Characterization, 105: 30-46
3. Manna A, Bhattacharayya B (2003) A study on machinability of Al/SiC-MMC. J Mater Process Technol 140:711–716 . doi: 10.1016/S0924-0136(03)00905-1
4. Ozben T, Kilickap E, Çakir O (2008) Investigation of mechanical and machinability properties of SiC particle reinforced Al-MMC. J Mater Process Technol 198:220–225 . doi:

10.1016/j.jmatprotec.2007.06.082

5. Li X, Seah WKH (2001) Tool wear acceleration in relation to workpiece reinforcement percentage in cutting of metal matrix composites. Wear 247:161–171 . doi: 10.1016/S0043-1648(00)00524-X
6. Pramanik A, Zhang LC, Arsecularatne J a. (2007) An FEM investigation into the behavior of metal matrix composites: Tool-particle interaction during orthogonal cutting. Int J Mach Tools Manuf 47:1497–1506 . doi: 10.1016/j.ijmachtools.2006.12.004
7. Bhushan RK, Kumar S, Das S (2010) Effect of machining parameters on surface roughness and tool wear for 7075 Al alloy SiC composite. Int J Adv Manuf Technol 50:459–469 . doi: 10.1007/s00170-010-2529-2
8. Ghani J, Haron C, Kasim M (2015) Wear mechanism of coated and uncoated carbide cutting tool in machining process. J Mater 1–7 . doi: 10.1557/jmr.2015.382
9. Li, J.; Liu, J.; Liu, J.; Ji, Y.; Xu C (2013) Experimental investigation on the machinability of SiC nano-particles reinforced magnesium nanocomposites during micro-milling processes Juan Li , Jian Liu , Jinling Liu , Yingfeng Ji and. 8:64–84
10. Teng X, Huo D, Wong E, et al (2016) Micro-machinability of nanoparticle-reinforced Mg-based MMCs: an experimental investigation. Int J Adv Manuf Technol 1–14 . doi: 10.1007/s00170-016-8611-7
11. Li P, Oosterling JAJ, Hoogstrate AM, et al (2011) Design of micro square endmills for hard milling applications. Int J Adv Manuf Technol 57:859–870 . doi: 10.1007/s00170-011-3330-6
12. Tansel I, Rodriguez O, Trujillo M, et al (1998) Micro-end-milling—I. Wear and breakage. Int J Mach Tools Manuf 38:1419–1436 . doi: 10.1016/S0890-6955(98)00015-7
13. Tansel I., Arkan T., Bao W., et al (2000) Tool wear estimation in micro-machining. Int J Mach Tools Manuf 40:599–608 . doi: 10.1016/S0890-6955(99)00073-5
14. Rahman M, Senthil Kumar a., Prakash JRS (2001) Micro milling of pure copper. J Mater Process Technol 116:39–43 . doi: 10.1016/S0924-0136(01)00848-2
15. Filiz S, Conley CM, Wasserman MB, Ozdoganlar OB (2007) An experimental investigation of micro-machinability of copper 101 using tungsten carbide micro-endmills. Int J Mach Tools Manuf 47:1088–1100 . doi: 10.1016/j.ijmachtools.2006.09.024
16. Ucun I, Aslantas K, Bedir F (2013) An experimental investigation of the effect of coating material on tool wear in micro milling of Inconel 718 super alloy. Wear 300:8–19 . doi: 10.1016/j.wear.2013.01.103
17. Imran M, Mativenga PT, Gholinia A, Withers PJ (2014) Comparison of tool wear mechanisms and surface integrity for dry and wet micro-drilling of nickel-base superalloys. Int J Mach Tools Manuf 76:49–60 . doi: 10.1016/j.ijmachtools.2013.10.002
18. Meenashisundaram GK, Gupta M (2014) Low volume fraction nano-titanium particulates for improving the mechanical response of pure magnesium. J Alloys Compd 593:176–183 . doi: 10.1016/j.jallcom.2013.12.157
19. Ramaswami R (1971) The effect of the built-up-edge(BUE) on the wear of cutting tools. Wear 18:1–10 . doi: 10.1016/0043-1648(71)90059-7
20. Friedrich CR, Kulkarni VP (2004) Effect of workpiece springback on micromilling forces. Microsyst Technol 10:472–477 . doi: 10.1007/s00542-004-0375-6